Segmentation on remote sensing images by using Fusion-MRF model*

Tamás Szirányi

*with Maha Shadaydeh

MTA SZTAKI Hungarian Academy of Sciences
Computer and Automation Research Institute

11/24/2015

1984

2000

2005

2007

Analysis Tasks in RS Image repositories

- Classifying segments and detection of changes in terrestrial areas are important and time-consuming efforts for remote-sensing image repositories.

- Some country areas are scanned frequently (e.g. year-by-year) to spot relevant changes, and several repositories contain multi-temporal image samples for the same area in very different quality and details.

Fused segmentation of the different subclasses




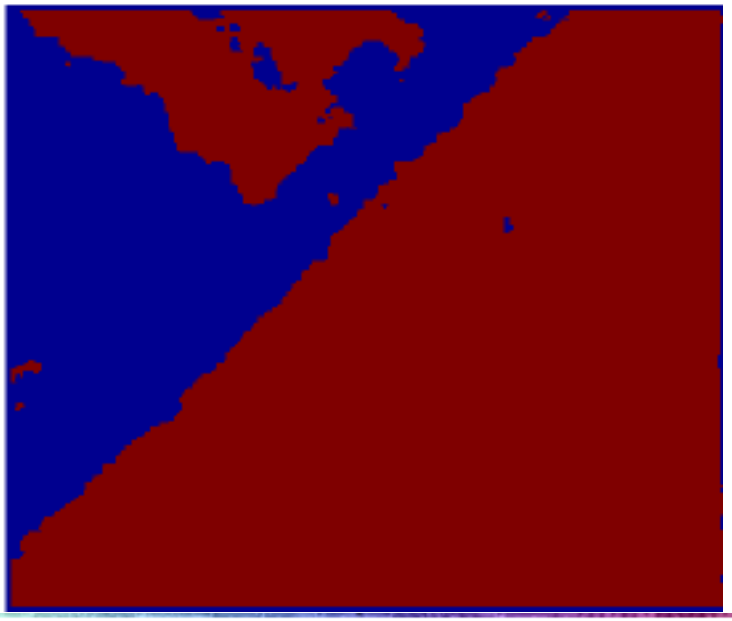

Outlines

- Objective and Background
- Multi-Layer Fusion MRF model for change detection in remote sensing images.
- Improved local similarity measure estimation algorithm
- Experimental Results on Wetland
- Conclusion

Objective and Background

- Land Cover Monitoring: Detecting regions of changes in remote sensing images that come from different sensors or different lighting and weather conditions.
- Development of Post Classification Comparison (PCC) approach for Change Detection.
  - Multi-temporal images is first segmented into various land-cover classes, like urban areas, wetlands, forests, etc.
  - Changes are then obtained as regions with different class labels in the different time layers.

Multi-Layer Fusion MRF Model[1]

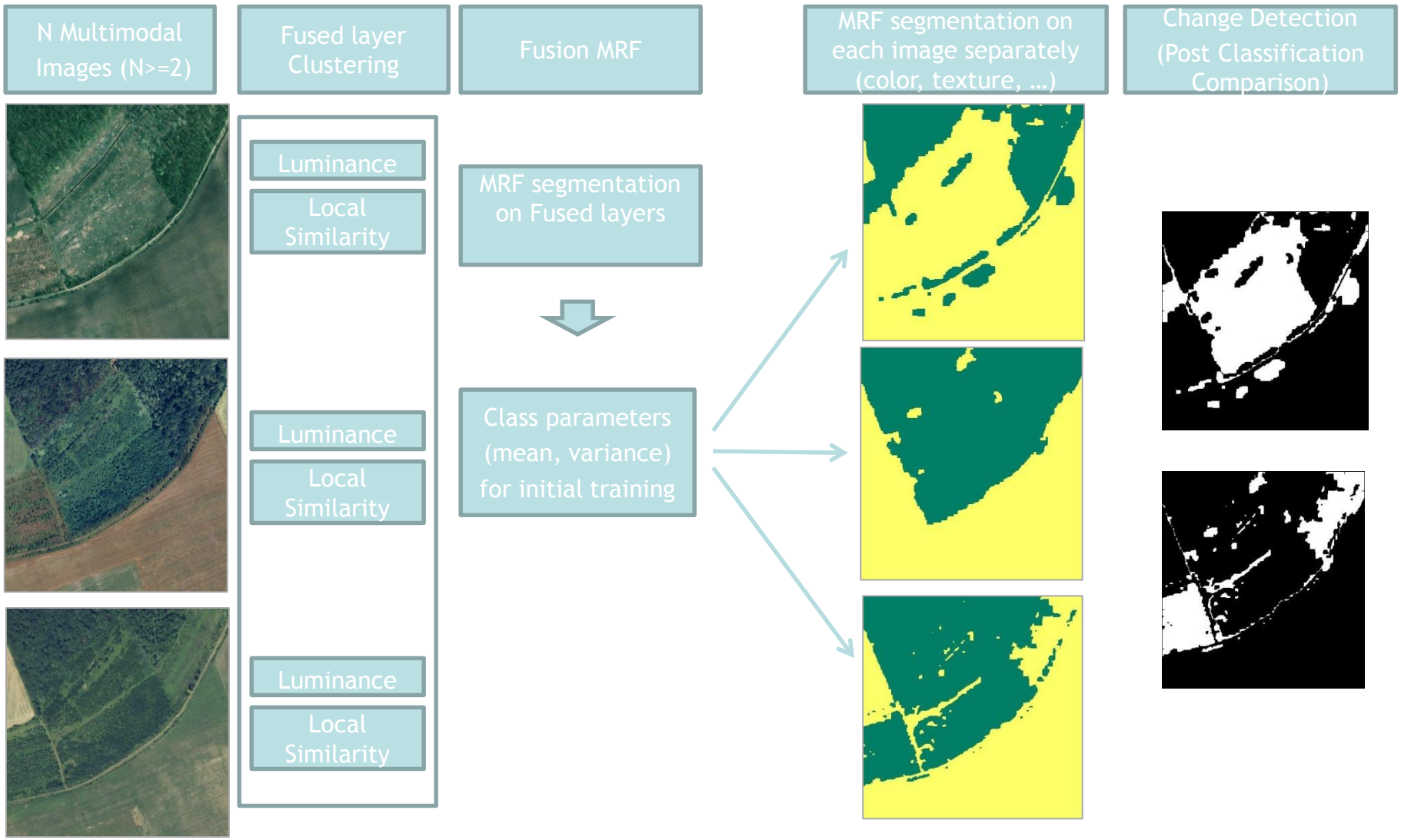

[1] *Sziranyi & Shadaydeh, IEEE GSRS Letters, 2014*

Proposed method:

- Color and texture features
- Cross-image featuring
- Multi-Layer Markovian adaptive fusion
- Single layer segmentation based on fusion clusters
- Segmentation and detection of changes

Detecting details in rarely scanned remote sensing areas, where trajectory analysis or direct comparison is not applicable.

Proposed steps:

- unsupervised or partly supervised clustering in fusion mode,
- cross-image featuring,
- multilayer MRF fusion segmentation in the mixed dimensionality;
- clusters of the single layers are trained by clusters of the mixed results.

Fused segmentation of the different subclasses




More images

More information

More complex details

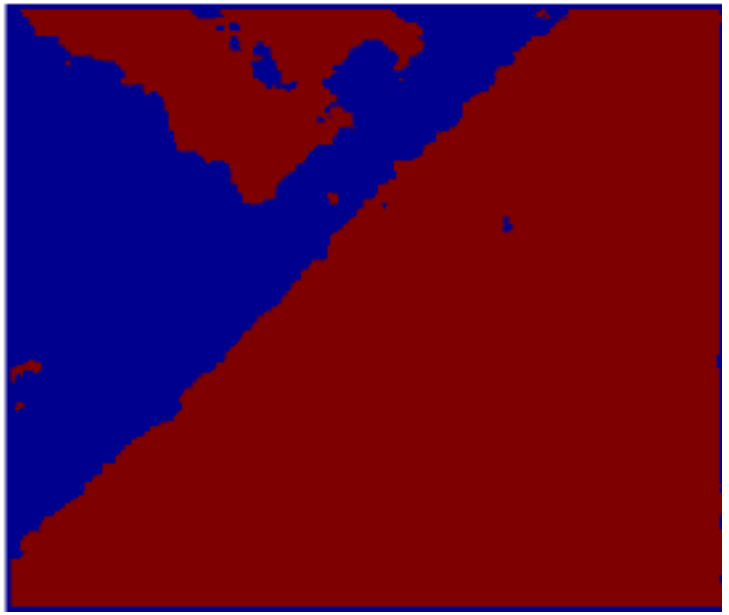

MRF models and segmentation levels:

- ***Single layer***

  single year – some supervision is needed

- ***Multiple layers*** **(stack of years' layers):**

  the source of supervision for single layer step

$$\widehat{\Omega} = \operatorname{argmin}_{\Omega} \sum_{s \in S} \underbrace{-\log P(\overline{x}_s | \omega_s)}_{\epsilon_{\omega_s}(s)} + \sum_{r,s \in S} \Theta(\omega_r, \omega_s)$$

$$\Theta(\omega_r, \omega_s) = \begin{cases} 0 & \text{if } \omega_r = \omega_s \\ +\beta & \text{if } \omega_r \neq \omega_s \end{cases}$$

Similarity Measures: cross-layer feature

- Change detection methods based on radiometry measurement alone are not useful when dealing with image time series data that comes from different sensors such as optical and synthetic aperture radar.
- In such case, similarity measures provide useful tool for change detection and image time series analysis.

Cluster Reward Algorithm (CRA)

For two images I and J the CRA is defined as:

$$CRA(I,J) = \frac{\sum_{i,j} p^2_{IJ}(i,j) - \sum_i p^2_I(i) \cdot \sum_j p^2_J(j)}{\sqrt{\sum_i p^2_I(i) \cdot \sum_j p^2_J(j)} - \sum_i p^2_I(i) \cdot \sum_j p^2_J(j)}$$

The denominator is a normalization term and the numerator contains terms that are similar to other similarity measures as distance to independence or mutual information. The main advantage of the CRA is that the joint histogram estimation noise has weak influence on the CRA values, thus smaller estimation window can be used.

CRA Calculation

I

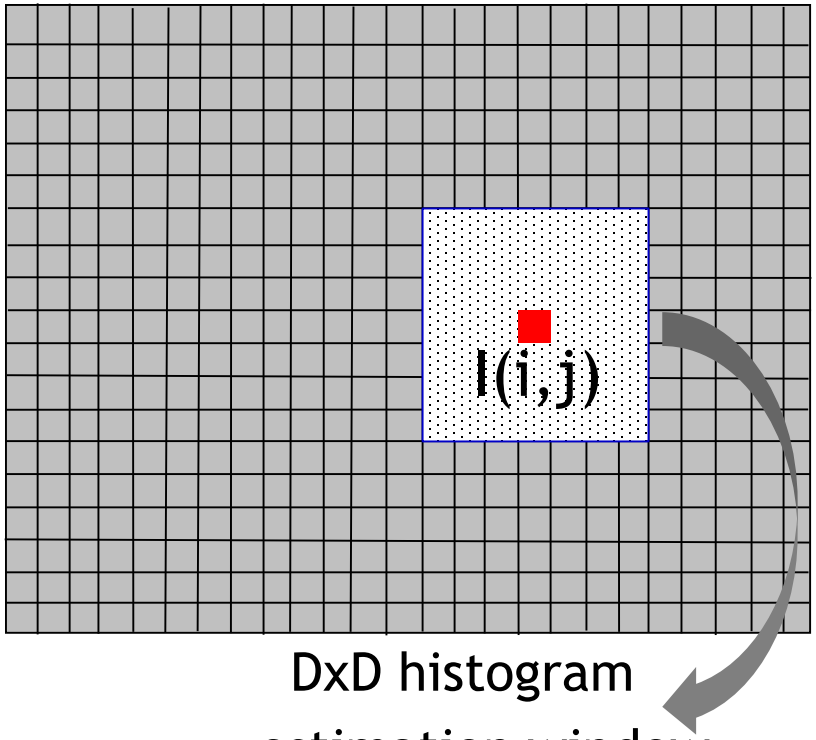

DxD histogram estimation window.

$$CRA(I,J) = \frac{\sum_{i,j} p^2_{IJ}(i,j) - \sum_i p^2_I(i) \cdot \sum_j p^2_J(j)}{\sqrt{\sum_i p^2_I(i) \cdot \sum_j p^2_J(j)} - \sum_i p^2_I(i) \cdot \sum_j p^2_J(j)}$$

J

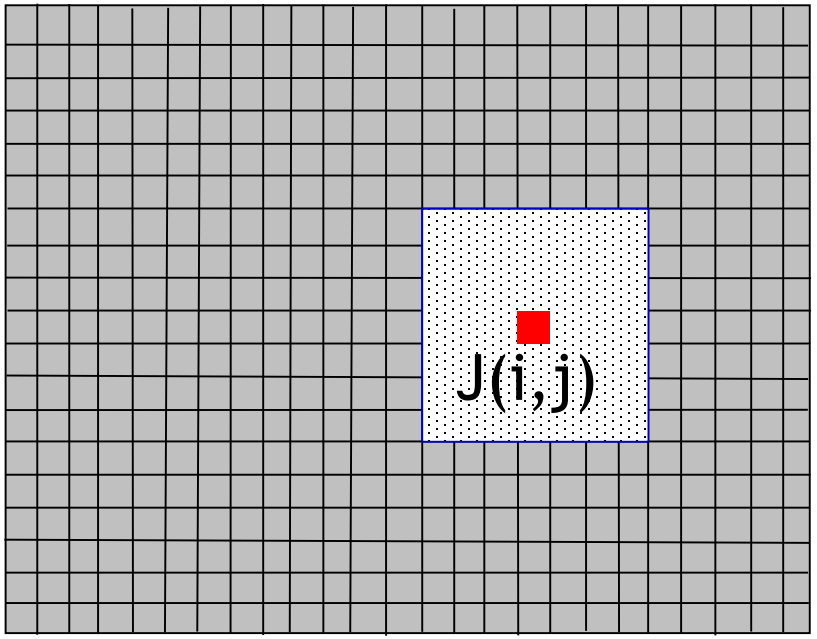

Marginal and joint histograms can be estimated from subsets of the images. The window size can be varied according to the required scale of change detection.

Local Similarity Measure Estimation

Cluster Reward Algorithm (CRA) Similarity Measure

$$CRA(I,J,s) = \frac{\sum_{i,j} p^2_{IJ}(i,j,w_s) - \sum_i p^2_I(i,w_s)\sum_j p^2_J(j,w_s)}{\sqrt{\sum_i p^2_I(i,w_s)\sum_j p^2_J(j,w_s)} - \sum_i p^2_I(i,w_s)\sum_j p^2_J(j,w_s)}.$$

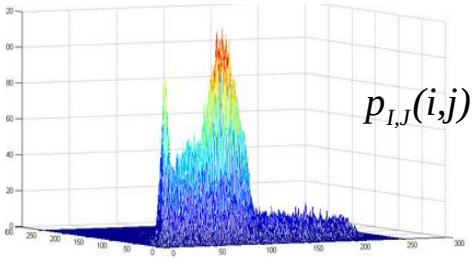

$$p_{I,J}(i,j) = \frac{h(i,j)}{\sum_{i,j} h(i,j)}$$

Joint local histogram h(i, j) of the two corresponding windows in images I and J

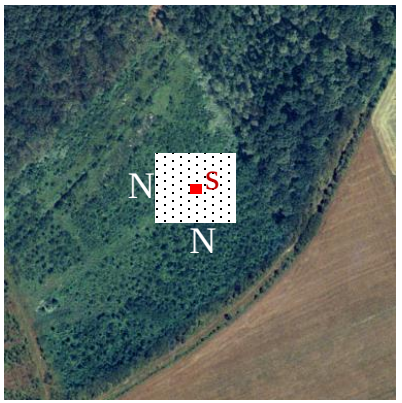

Image I

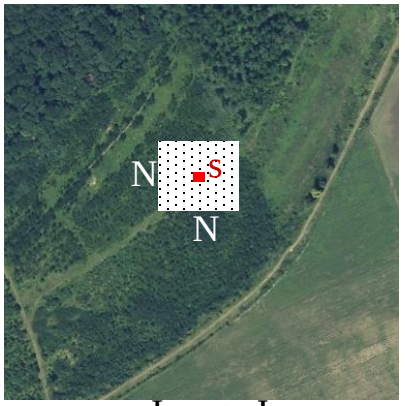

Image J

Problem: Choice of window size N.

- Large window provide better estimation for the pdfs, but can not detect smaller changes.
- Small window gives large estimation error.

Cross-layer similarity measures

The main idea in the proposed algorithm is to apply the multilayer fusion MRF on CRA images calculated for each pair in a series of remote sensing images.

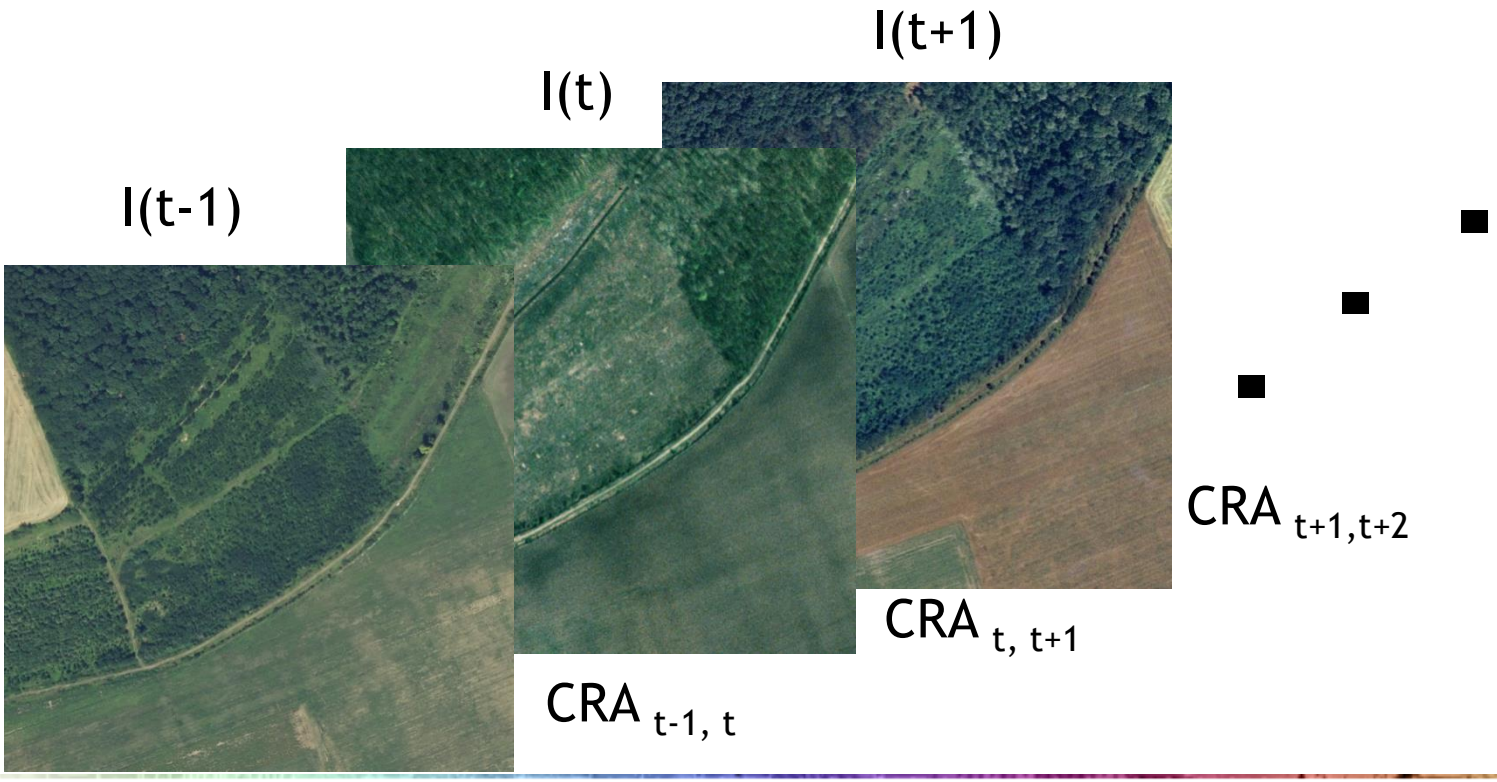

Proposed Algorithm

1. Selecting and registering the image layers.
2. For each pair of the three consecutive images I(t -1); I(t); I(t + 1), the CRA image is calculated using NxN estimation window around each pixel; then normalized to have values in the range [0; 1].
3. In the color space Luv, let $x_t(s)$ denotes the L color value of pixel s in image I(t). Construct a combined feature vector for pixels s in the three images I(t -1); I(t); and I(t + 1):

$$\overline{x_t}(s) = [x_{t-1}(s) + \alpha CRA_{t-1,t}(s), \overline{x}_t(s) + \alpha CRA_{t,t+1}(s), \\ x_{t+1}(s) + \alpha CRA_{t+1,t+2}(s)\,]$$

α is an adaptive positive weight.

Proposed Algorithm (cont.)

4. Defining training areas. Evaluating the $(\overline{x}_t(s))$ vectors on the training areas, the statistical data (mean and covariance) for the fusion based clusters are given; Note that this step can be replaced with *K-means* clustering for unsupervised segmentation.
5. Running MRF segmentation on the fused layer data $(\overline{x}_t(s))$resulting in a multilayer labeling $\Omega_{t-1;t;t+1}$;
6. Single-layer training: the multilayer labeling $\Omega_{t-1;t;t+1}$ is used as a preliminary training map for each image.
7. For each single layer a MRF segmentation is processed, resulting in a labeling Ω_t; In this step, the feature vector of each pixel consists of its three Luv color values only.

Forest / Meadow changes: 2000 - 2005 - 2007

Unsupervised segmentation and change detection by using texture and color info

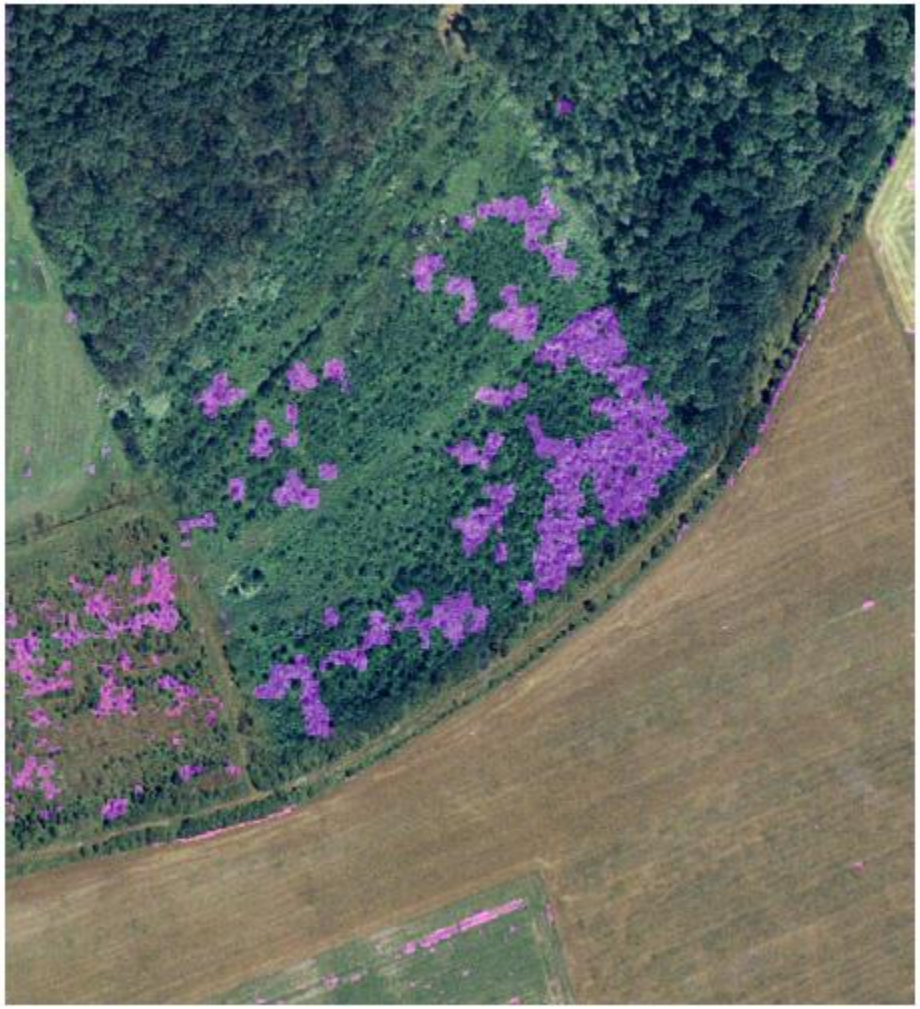

Unsupervised segmentation and change detection by using CRA cross-layer measure and color info

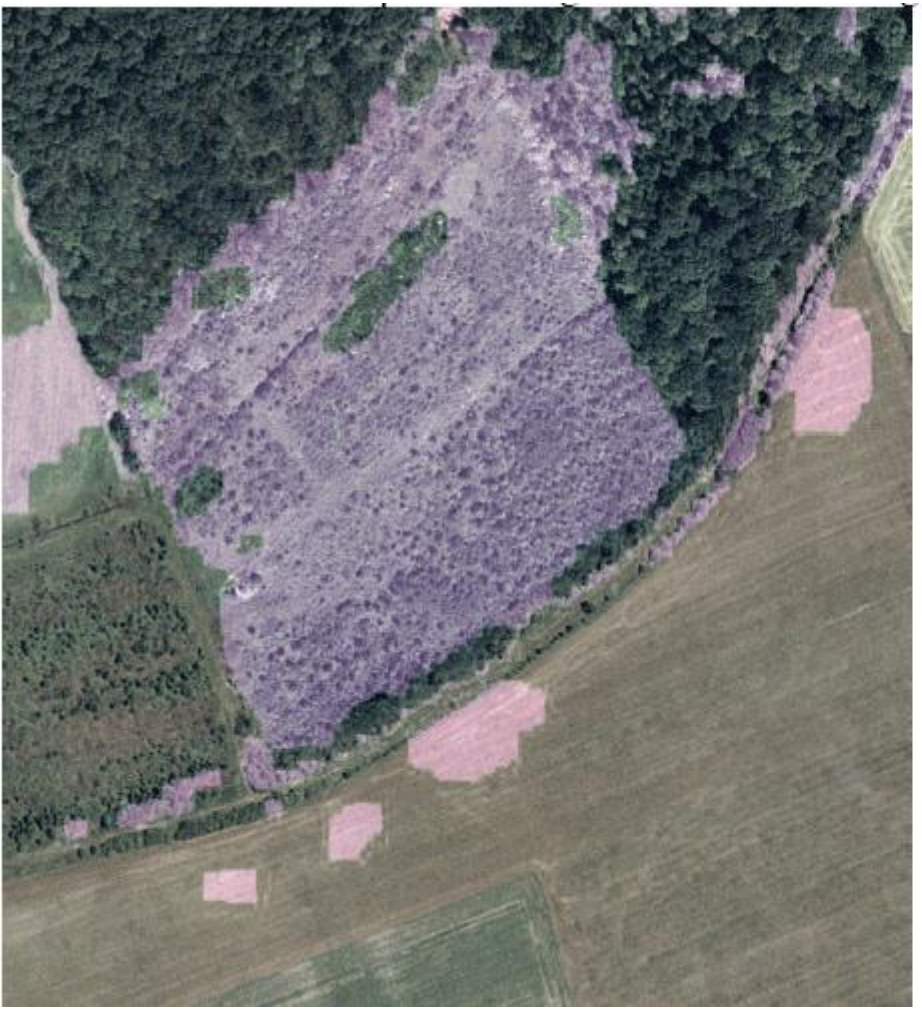

Experiment results

We compare the performance of four methods:

1) single layer MRF optimization on Luv color values on the separate layers (SL-MRF)
2) single layer MRF optimization on Luv color values on the separate layers and CRA similarity measure values among the layers (SL-MRF-CRA)
3) The proposed multilayer fusion MRF on Luv color values only (ML-MRF)
4) The proposed multilayer fusion MRF on color values and the CRA similarity measure values among layers (ML-MRF-CRA).

Training areas used in the segmentation process

Meadow (M), Forest (F), Sand (S), and River (R) *in the Tiszadob area (by FÖMI)*

Row (1): aerial photos around the Tiszadob oxbow area (Hungary, photos by FO¨MI) from the years 2000, 2005 and 2007. Training areas used in the segmentation process are shown in the upper right image, Meadow (M), Forest (F), Sand (S), and River (R).

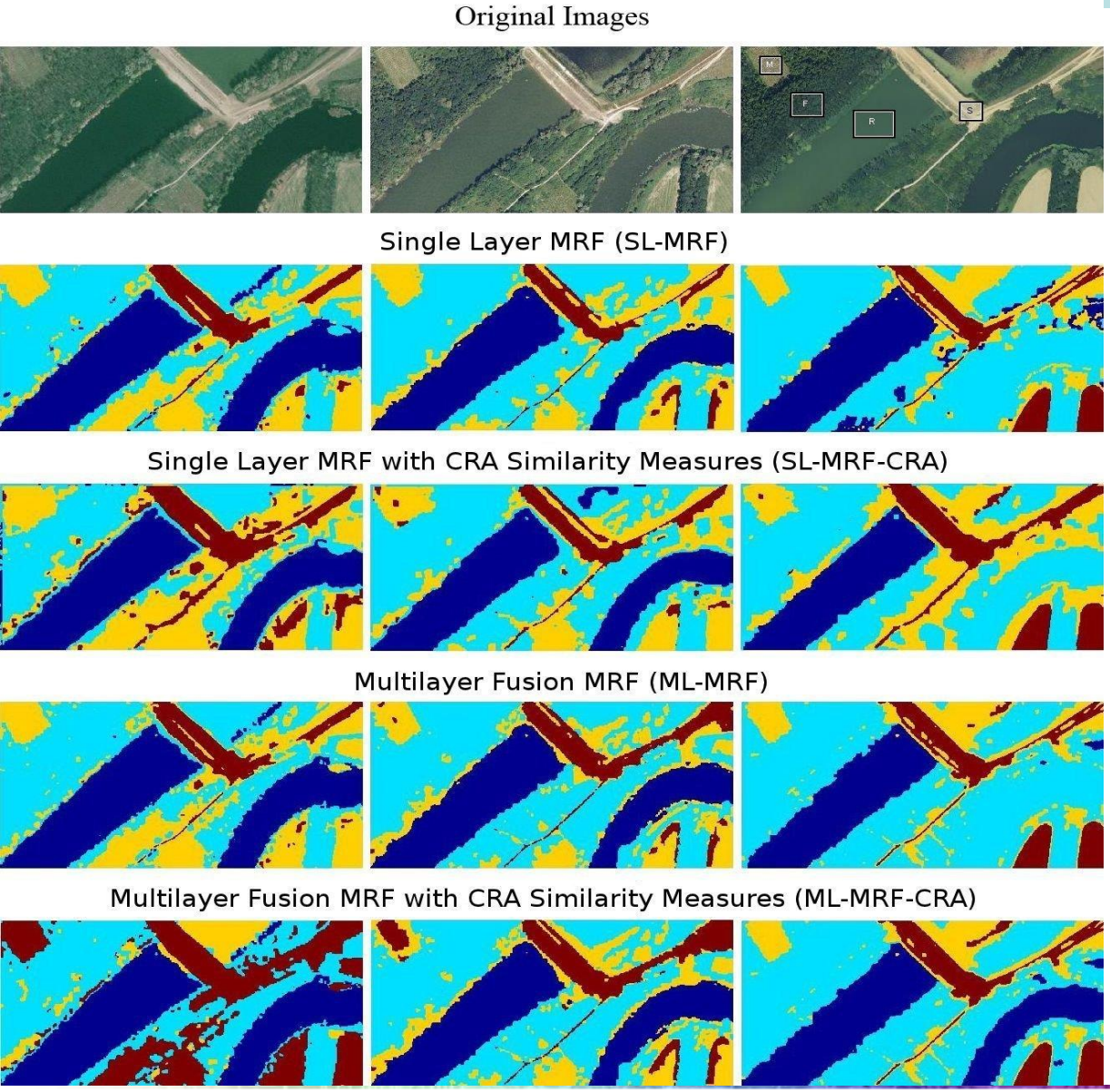

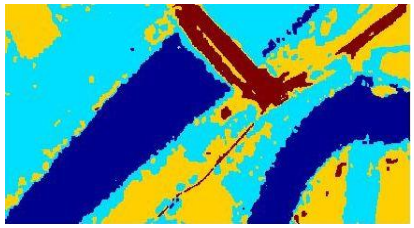

Ground-Truth result by a one layer fusion with infrared image.

Method	Misclassified pixels' rate
SL-MRF	19%
SL-MRF-CRA	20%
ML-MRF	21%
ML-MRF-CRA	10%

see oxbow section on the right

Experiment 1: Segmentation Results (cont.)

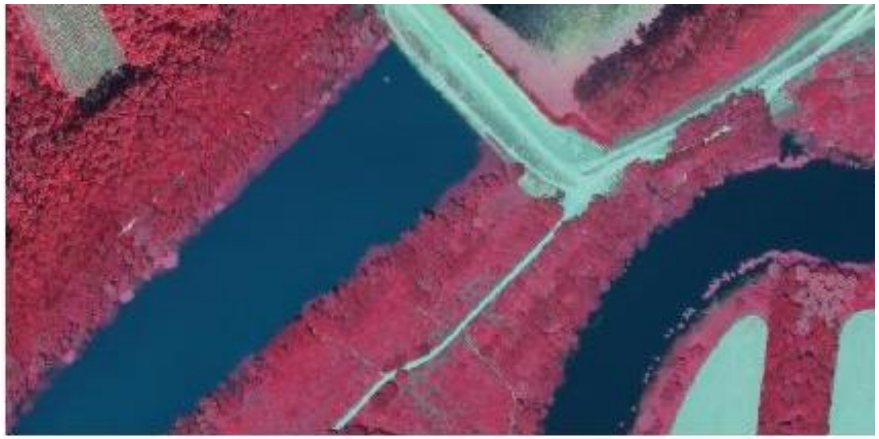

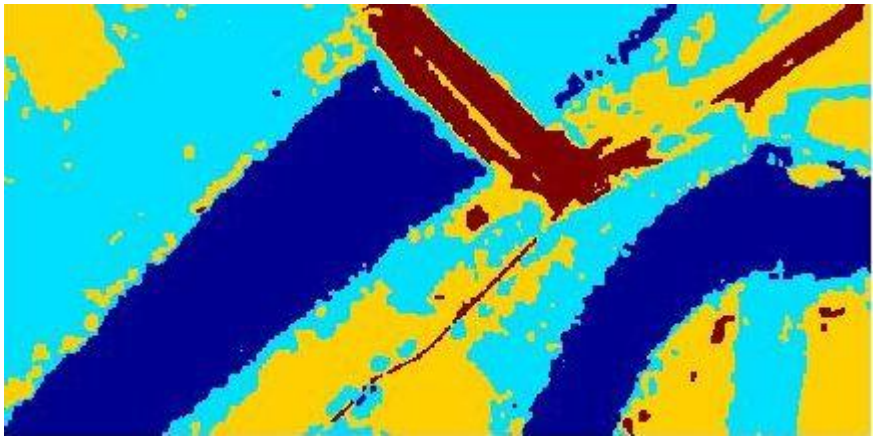

Ground-Truth result by a one layer fusion with infrared image to find a subclass (different water covers): Infrared image from the year 2007 (Left) and the segmentation results for 2007 (Right) using single layer MRF on Luv color values - see the oxbow on the right

Experiment 2: Segmentation Results on Ground-Truth samples (unsupervised using K-means)

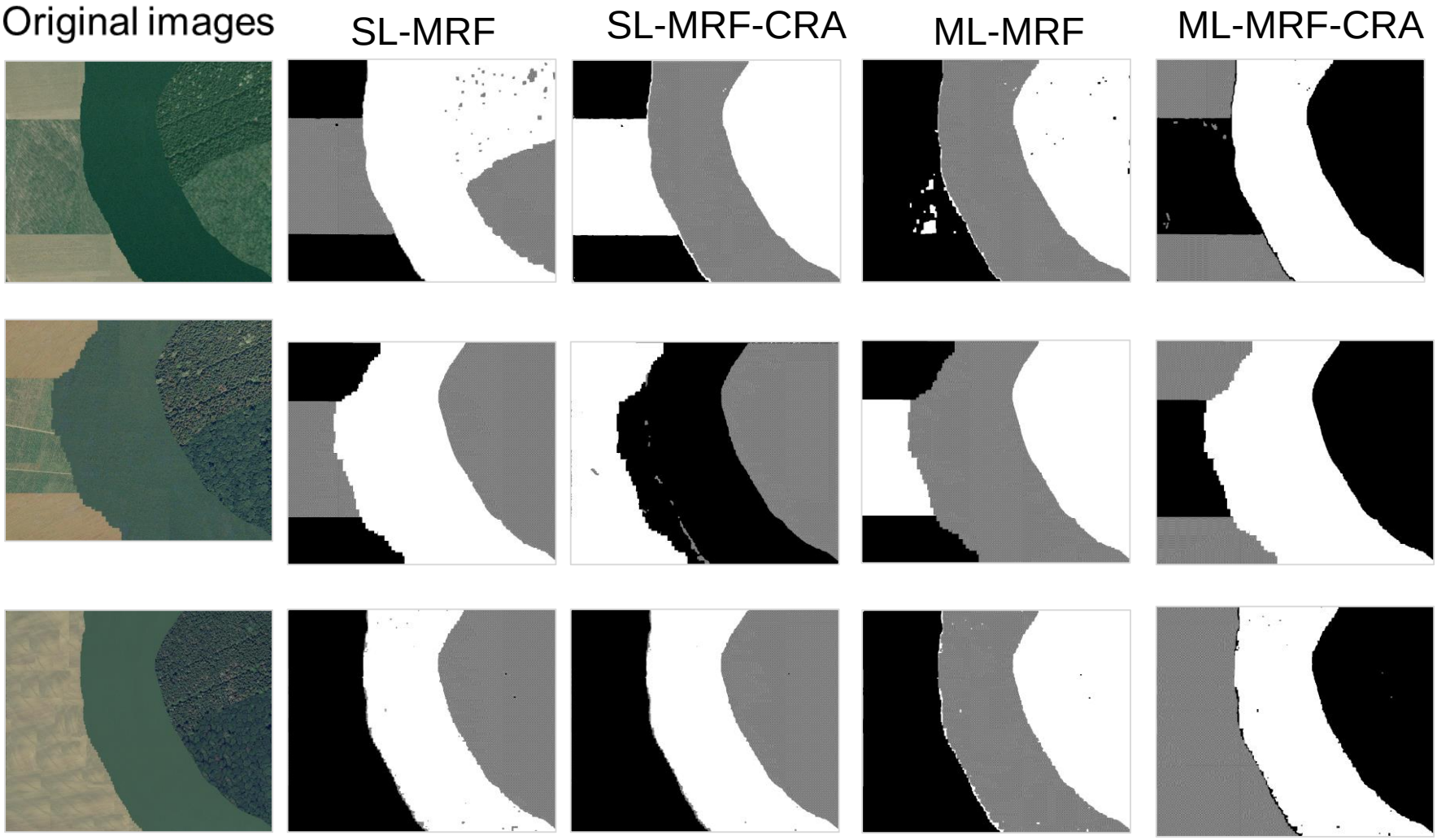

Experiment 2: Change Detection Results on Ground-Truth (unsupervised using K-means)

Original images

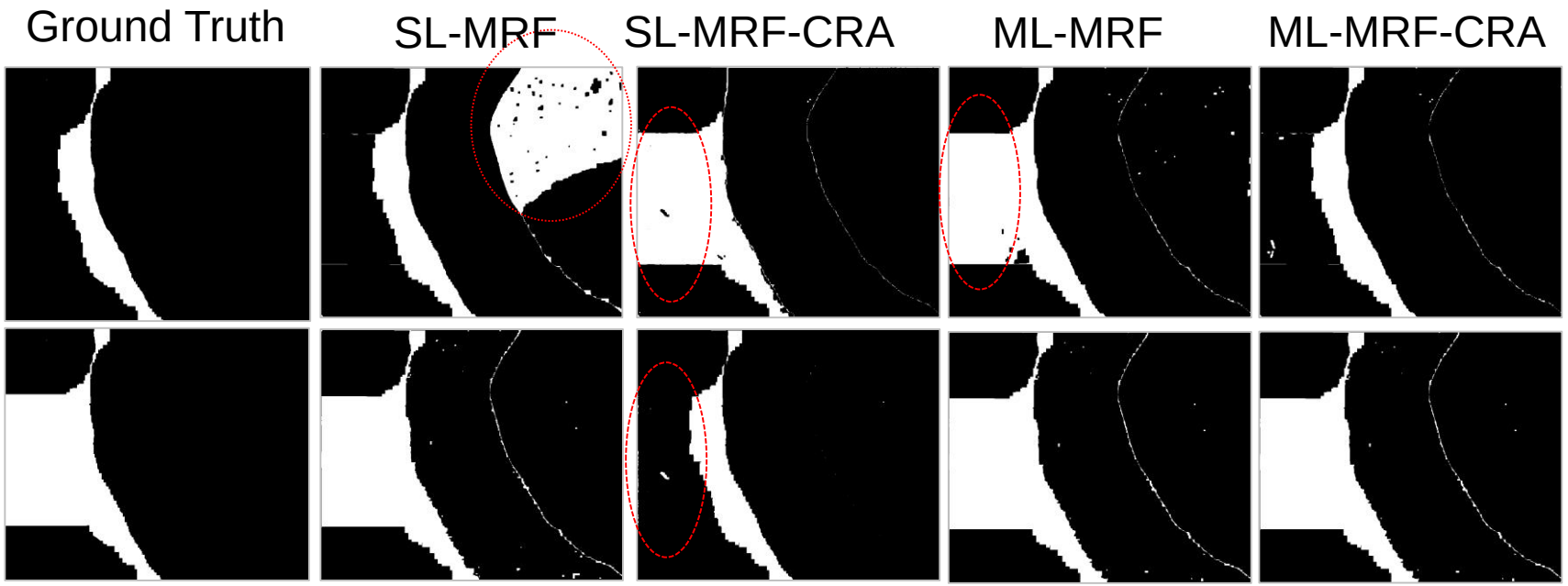

Circled areas denote misclassified regions.

Misclassified Pixels

Method	Sup.Segment. 2007, Fig.1	Unsup.Change Det, Fig.4 2003-2005	Unsup.Change Det, Fig.4 2005-2007	Time sec
SL-MRF	19%	16.4%	10.4%	43
SL-MRF-CRA	20%	11.3%	11.2%	293
ML-MRF	21%	11.04%	1.0%	52
ML-MRF-CRA	10%	0.65%	1.0%	290

Measuring the correlation term more effectively:

Registration process and Fusion term

An Improved Mutual Information Similarity Measure for Registration of Multi-Modal Remote Sensing Images

SPIE 2015, Toulouse and Wetland WS in Seville, 2015

Image Registration

Key points based techniques: Minimize the distance between the corresponding features in the two images.

Area-based techniques: Quantify similarity measure.

Intra-modal Images: Minimize the distance between the images intensity values using similarity measures such as mean square error or normalized cross-correlation.

Inter-modal Images: Minimize the distance between the images' intensity probability distributions.

- Normalized Mutual Information (NMI).
- Kullback-Leibler Distance.

Image Registration using MI

MI measures statistical dependency between two data-sets X and Y using their joint and marginal entropies

$$MI(X,Y) = H(X) + H(Y) - H(X,Y)$$

$$H(X) = \sum_{x} - P_X(x) \cdot \log P_X(x)$$

$$H(Y) = \sum_{y} - P_Y(y) \cdot \log P_Y(y)$$

$$H(X,Y) = \sum_{x,y} - P_{X,Y}(x,y) \cdot \log P_{X,Y}(x,y)$$

MI is maximum when the data-sets are geometrically aligned.

$$P_{x,y}(X,Y) = \frac{h(x,y)}{\sum_{x,y} h(x,y)}$$

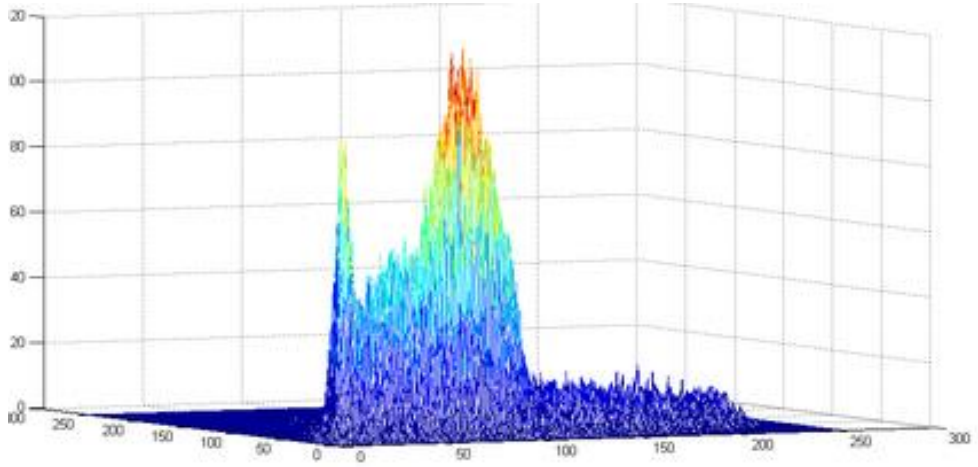

The joint histogram h(x, y) of two images X and Y equals the number of times the intensity pair (x, y) occurs.

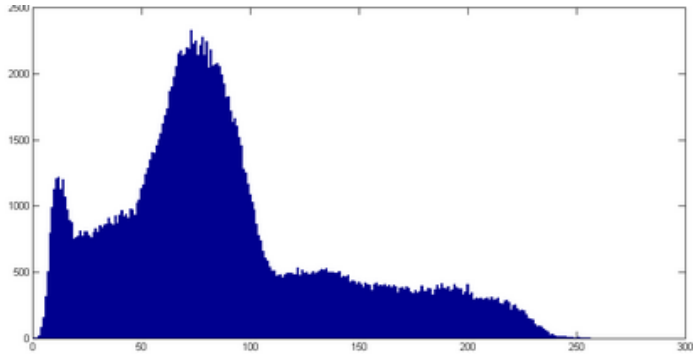

$$P_x(X) = \sum_y P_{X,Y}(x,y)$$

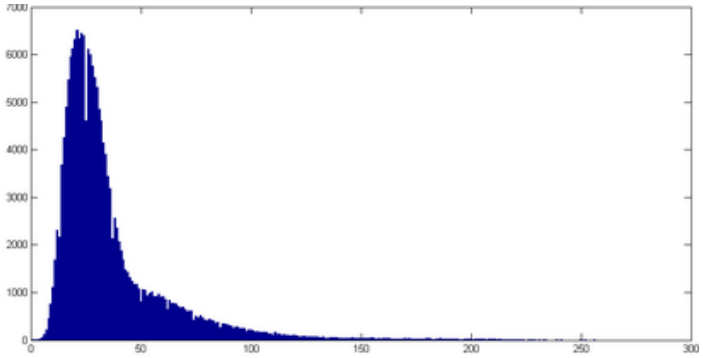

$$P_x(Y) = \sum_x P_{X,Y}(x,y)$$

Image Registration Using MI: Drawbacks

- MI surface is highly non-convex (many local max.)
- Spatial information is lost in the global MI.
- Sensitivity to number of bins used in histogram estimation
- Sensitivity to overlap region.
  - Normalized Mutual Information *(NMI)*

$$NMI(X,Y) = \frac{H(X)+H(Y)}{H(X,Y)}$$

Weighted Joint Histogram

The weight $\omega(s)$ given to each pixel s in the reference image is

$$\omega(s) = e^{-k.d(s)/g(s)}$$

k positive constant.

$g(s)$ normalized gradient image: use LoG filter

$d(s)$ distance image: Euclidean distance from the closest key-point.

Reference Image

weight map, key-points marked in red

Registration by WJH-MI: Experimental Results-1

Szada, Hungary in 1984, 1.5m/pixel.

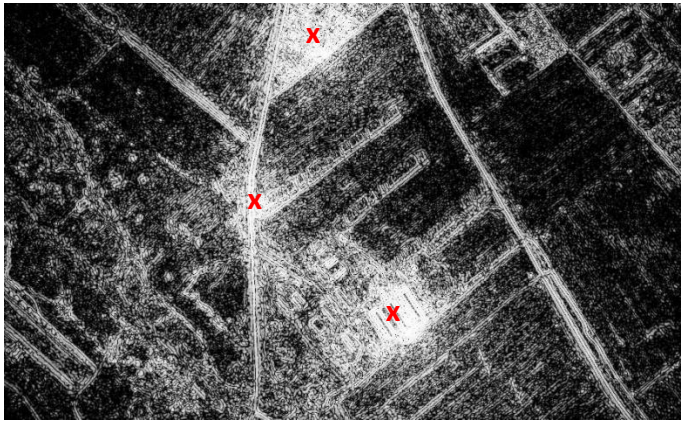

Weight map

Normalized gradient image calculated using LoG filter [σ=1, N=7].

Szada, Hungary in 2007. 1.5m/pixel.

True transformation parameters: horizontal translation T_h = 63 ; vertical translation T_v= 39;

rotation angle α = -4◦.

Search space: T_h = 20 : 1 : 70 (pixels),

T_v= = 20 : 1 : 70 (pixels), α = -7 : 1 :-1 (degree).

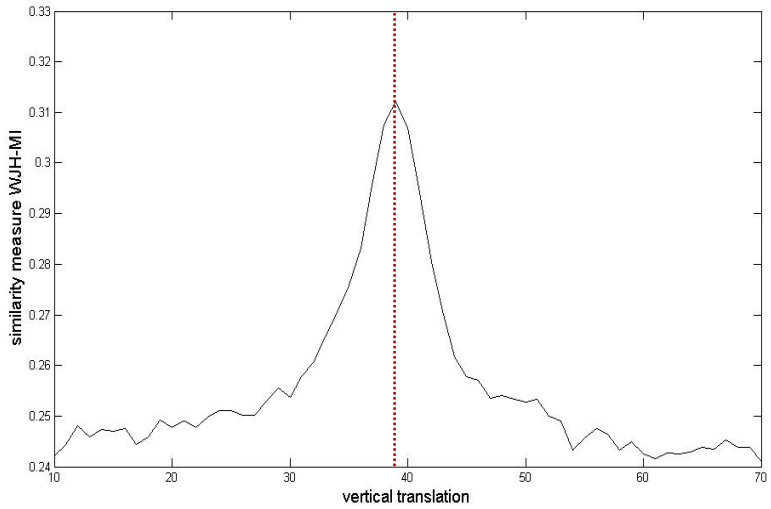

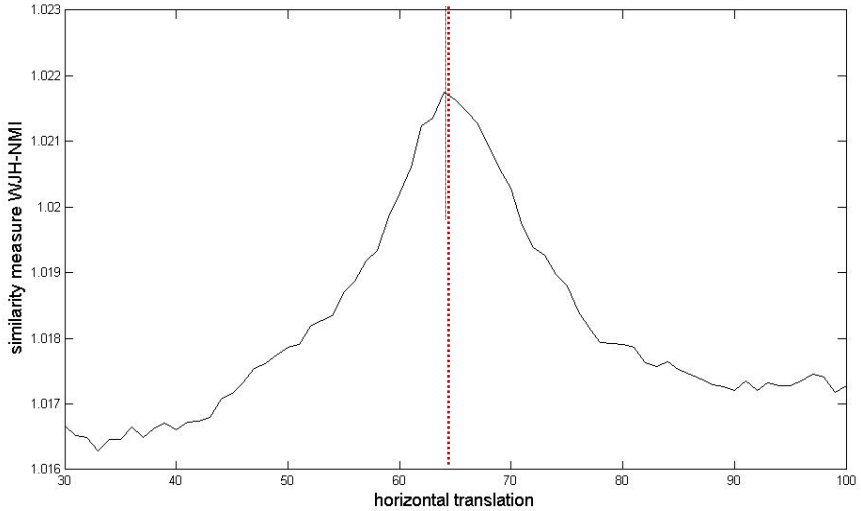

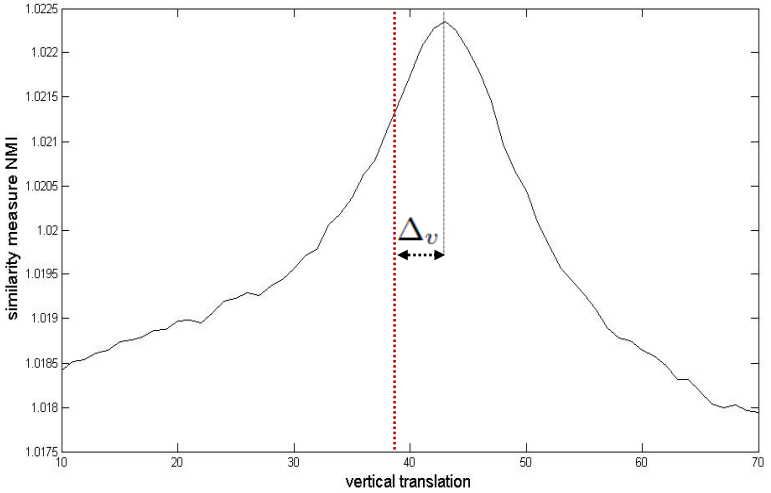

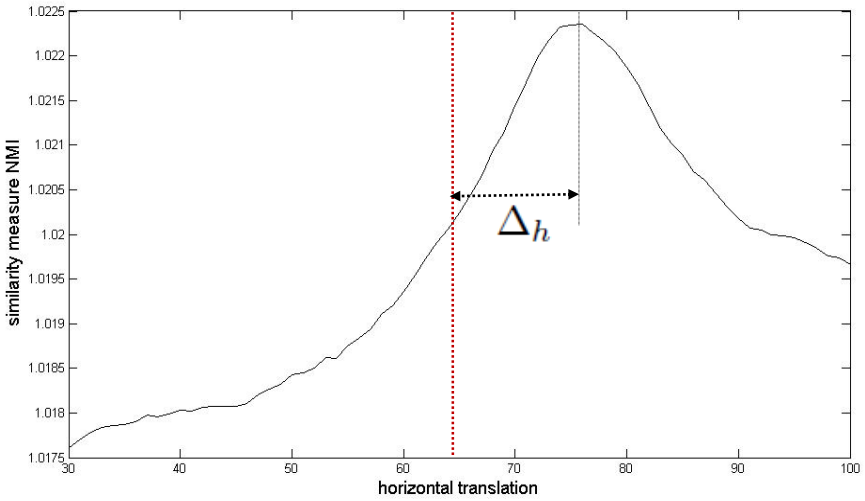

Vertical translation estimation error $\Delta_v = T_v - \hat{T}_v$ (pixels)

Horizontal translation estimation error $\Delta_h = T_h - \hat{T}_h$(pixels),

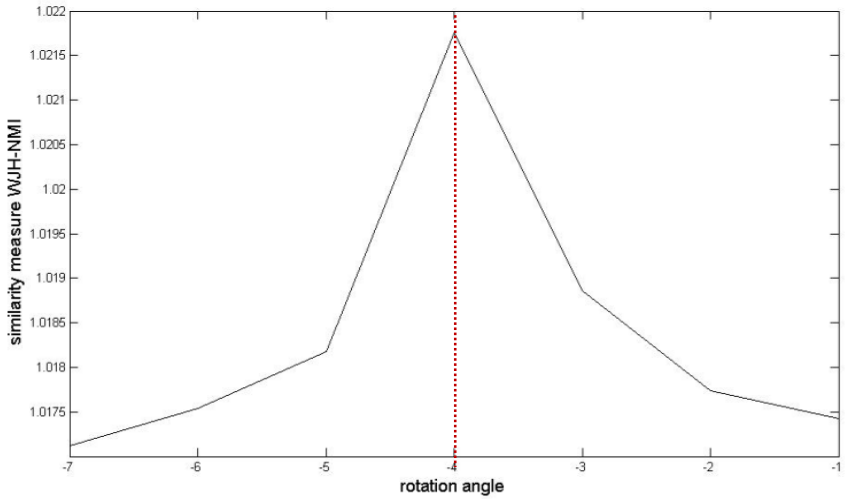

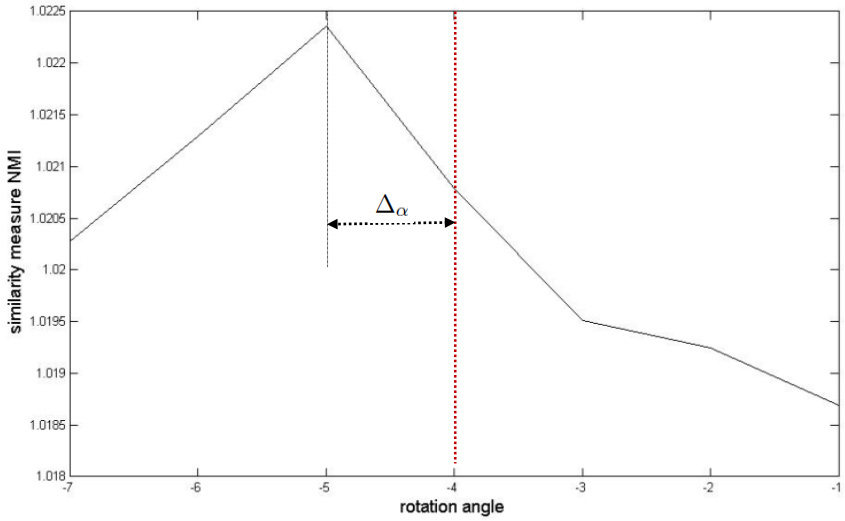

Rotation angle estimation error $\Delta_\alpha = \alpha - \hat{\alpha}(degree)$.

Registration by WJH-MI: Weight map

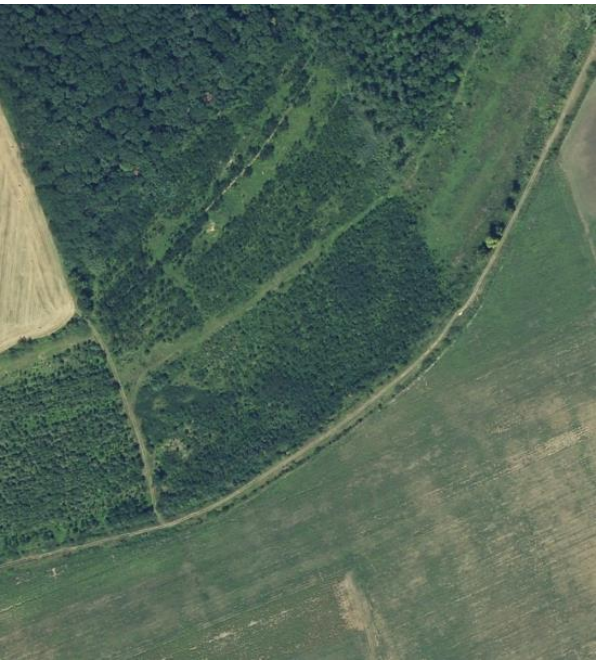

Szada area, 2007

Szada area, 2000.

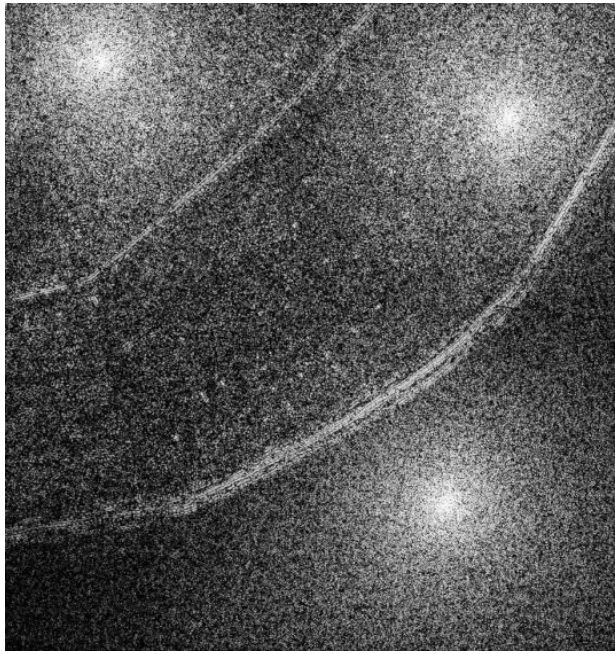

Weight map

Optimization using Gaussian pyramid (coarse to fine resolution).

Registration by WJH-MI: Experimental Results

registered images
using NMI

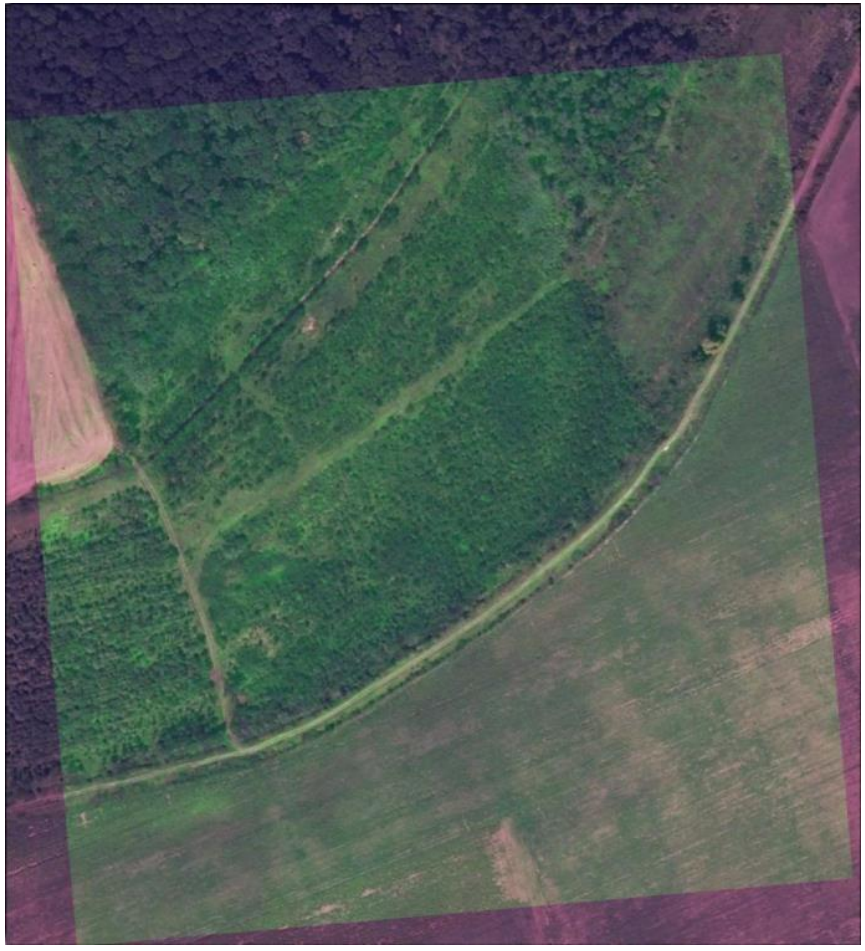

registered images
using WJH-NMI

Registration by WJH-MI: Convergence surface

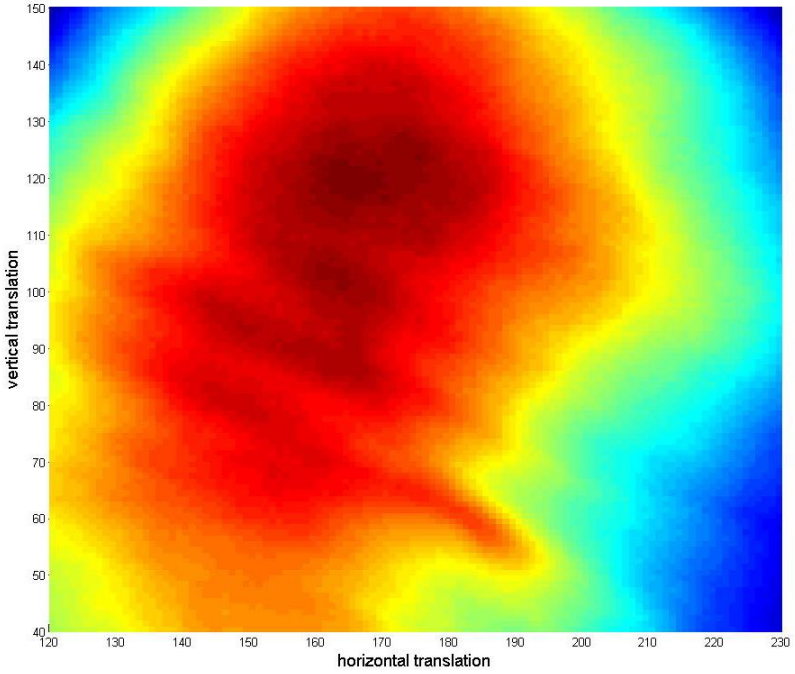

using NMI

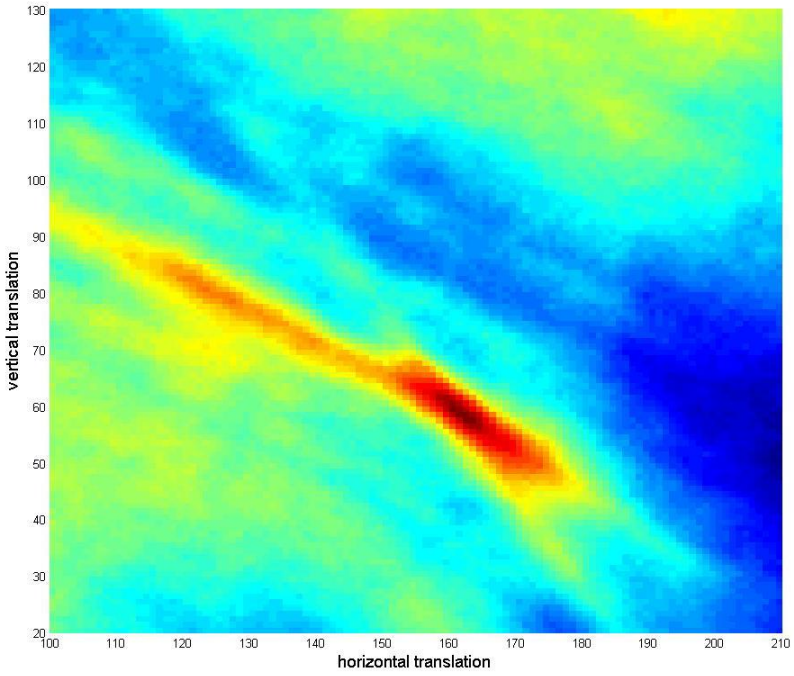

using WJH-NMI.

Contour plots of similarity measure convergence surface

Proposed Weighted Histogram Estimation in F-MRF

The weight given to each pixel s in the reference image is

$$\omega(s) = e^{-k.d(s)/g(s)}$$

k positive constant.

$g(s)$ initial change image: variance change ratio.

$d(s)$ Euclidean distance from the center of the window.

Tiszadob image year 2005

Tiszadob image year 2007

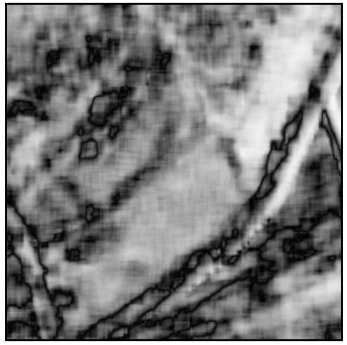

Initial change map: variance change ratio.

Change detection results using conventional CRA similarity measure.

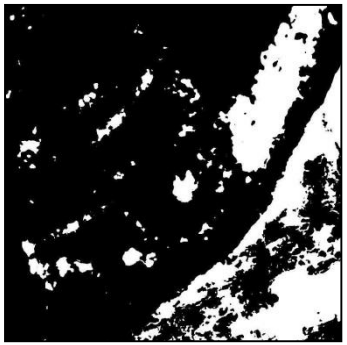

Change detection results using proposed CRA similarity measure.

Experimental Results for Wetlands

Exp. 2 – Monitoring Reed in Wetlands

Data set

Two Multi-Spectral (RGB and NIR) Pleiades images of Keszthely area, Hungary

Years: 2012, 2015.

Spatial resolution: 2 m/pixel

Method

- Unsupervised K-means clustering
- Classification using two layers fusion MRF on NDVI values + NIR channel + Luminance component.
- Single Layer MRF on each single layer.
- Post Classification Comparison for Change Detection

Keszthely (Aug. 2012)

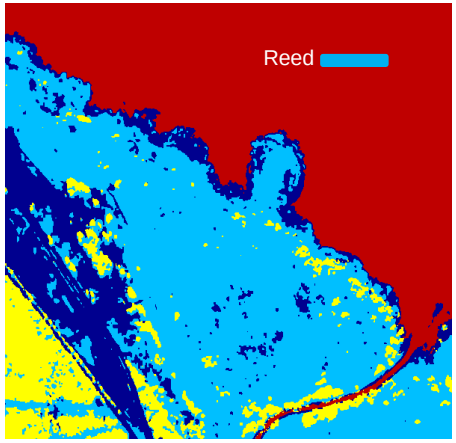

Segmentation results (2012).
Misclassified pixels' rate=7%
(compared to 2010 ground truth)

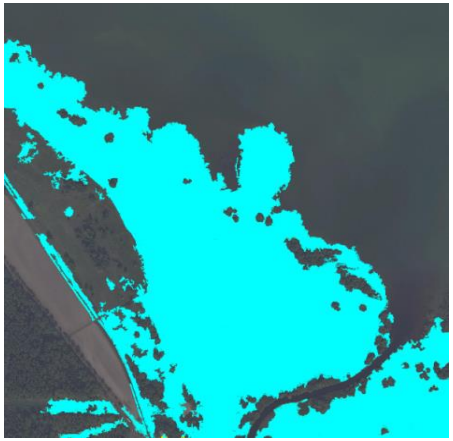

Reed Ground Truth (2010)
(Courtesy of A. Zlinszky)

Keszthely (June 2015)

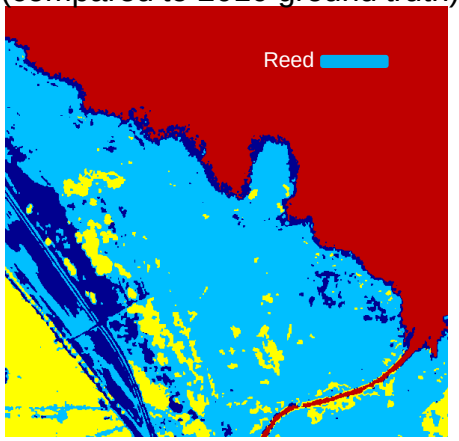

Segmentation results (2015)

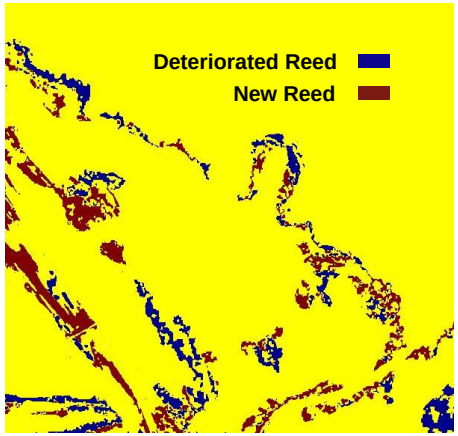

Change detection results between
years 2012 and 2015.

Experimental Results

Exp. 3 – Monitor dam construction effect on river Parana

Data set

Three Landsat RGB images of Parana river in Paraguay

Years: 1985, 1999, and 2010.

Dam construction starts in 1983.

Method

We apply the proposed multilayer fusion MRF on RGB values.

- Unsupervised K-means clustering
- Multi-layer FMRF on RGB values
- Single layer MRF segmentation for each layer on RGB values
- Post Classification Comparison for Change Detection

original images

segmented images

Change maps

1985

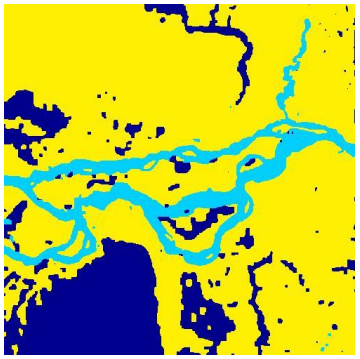

1999

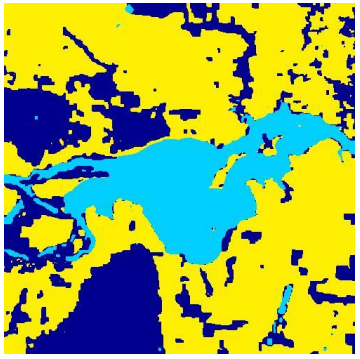

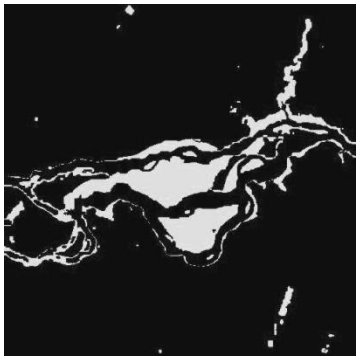

1985-1999

2010

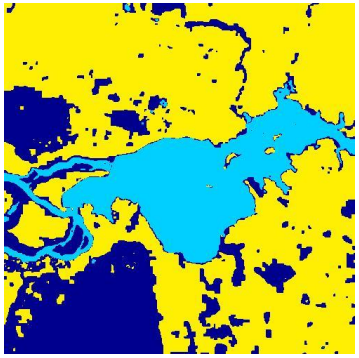

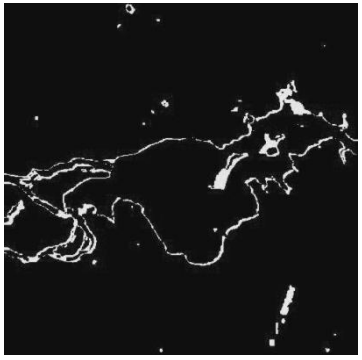

1999-2010

Conclusions

- A multi-temporal fusion MRF model is introduced and used for classification and change detection of wetlands in remote sensing image series.
  - MRF segmentation on the fused layer data resulting in a multi-layer labeling.
  - The multi-layer labeling is used as a training map for MRF segmentation of each single layer.
  - The consecutive image layers labeling are compared for change detection.
- Different spectral, spatial, and statistical features can be used in the ML-FMRF based on application. The use of cross-layer similarity for example helps to better identify some classes where radiometric values are dubious in Exp. 1., while the fusion of two layers NDVI index results in considerable improvement in reed classification.
- Since the outcome classes of the multi-layer segmentation is later used in the training of each single layer, similar classes are automatically given similar labels in all layers. This helps to define type as well as location of changes.

What is the change?
Returning to the basic question

Multilayer Markov Random Field models for change detection in optical remote sensing images

by

Csaba Benedek, Maha Shadaydeh, Zoltan Kato, Tamás Szirányi, Josiane Zerubia; in **ISPRS JPRS**, 2015

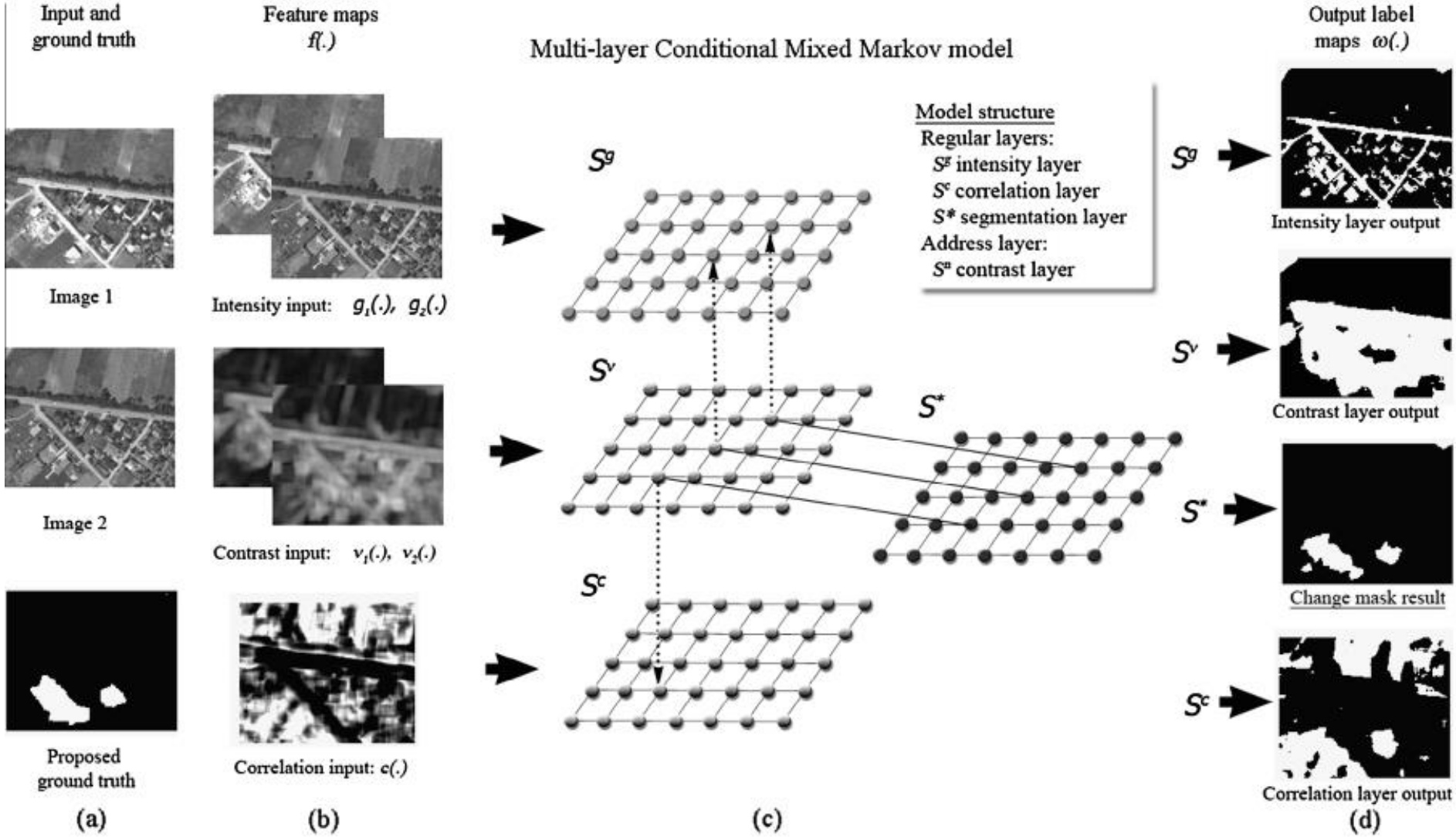

Structure of the CXM model and overview of the segmentation process.

Benedek&Sziranyi, IEEE TGRS, 2009

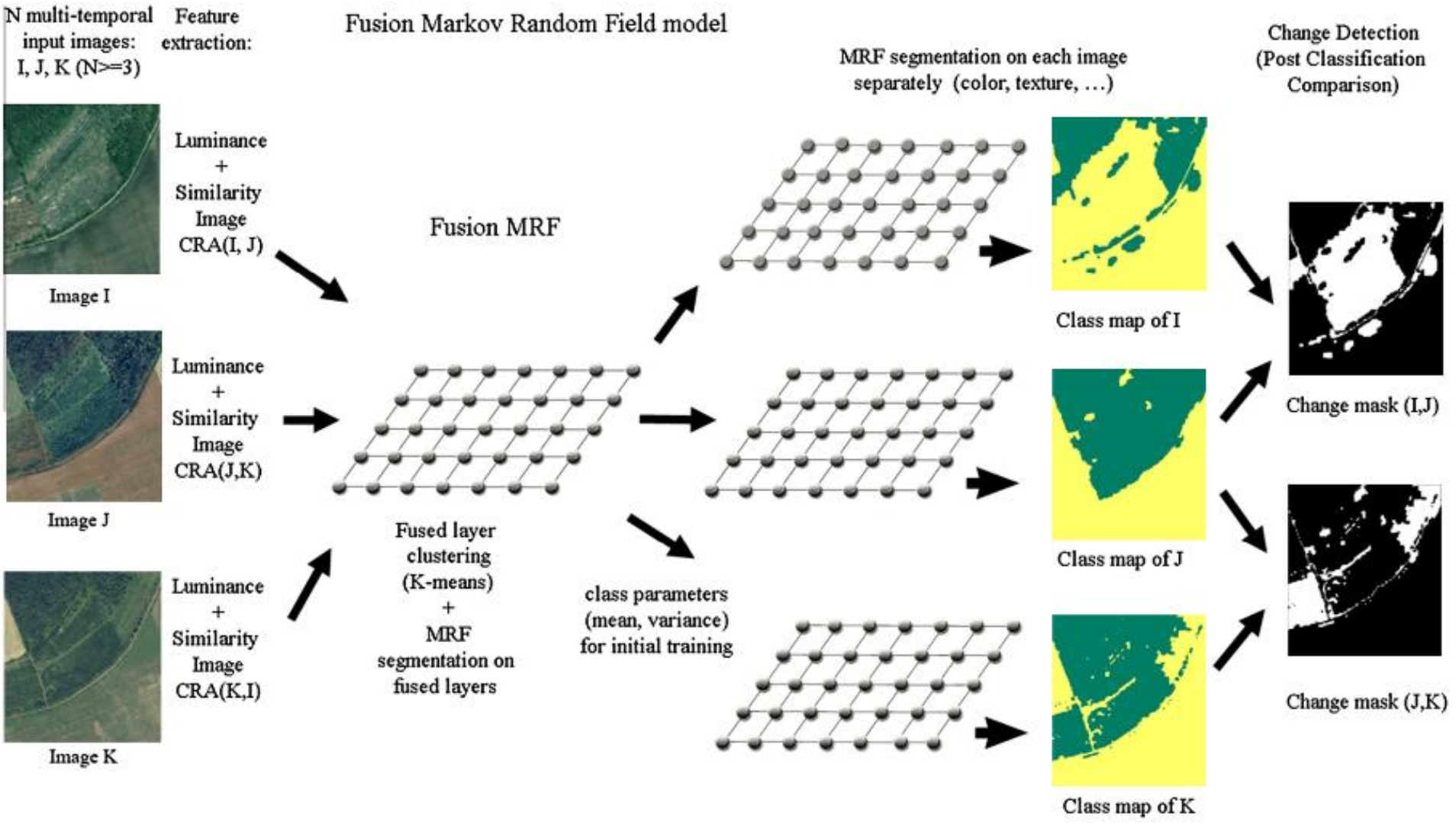

Structure of the FMRF model and workflow of the implemented Post-Classification Comparison process.

(a) Image from 2000: G_1 reference

(b) Image from 2005: G_2 reference

(c) Image from 2007 – only used by FMRF

(d) AirChange Ground Truth (G_1 vs. G_2)

(e) Region PCC Ground Truth (G_1 vs. G_2)

(a) Image from 2000: G_1 reference

(b) Image from 2005: G_2 reference

(c) Image from 2007 – only used by FMRF

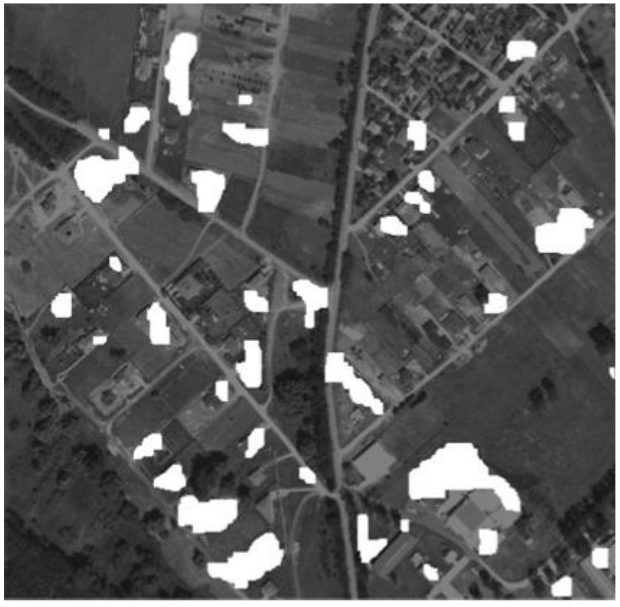

(f) L_3MRF result (G_1 vs. G_2)

(g) CXM result (G_1 vs. G_2)

(h) FMRF result (G_1 vs. G_2)

Difference between the obtained change masks: the large change area of CXM corresponds to a hardly visible fresh plough land

(a) Image 1: G_1 (b) Image 2: G_2

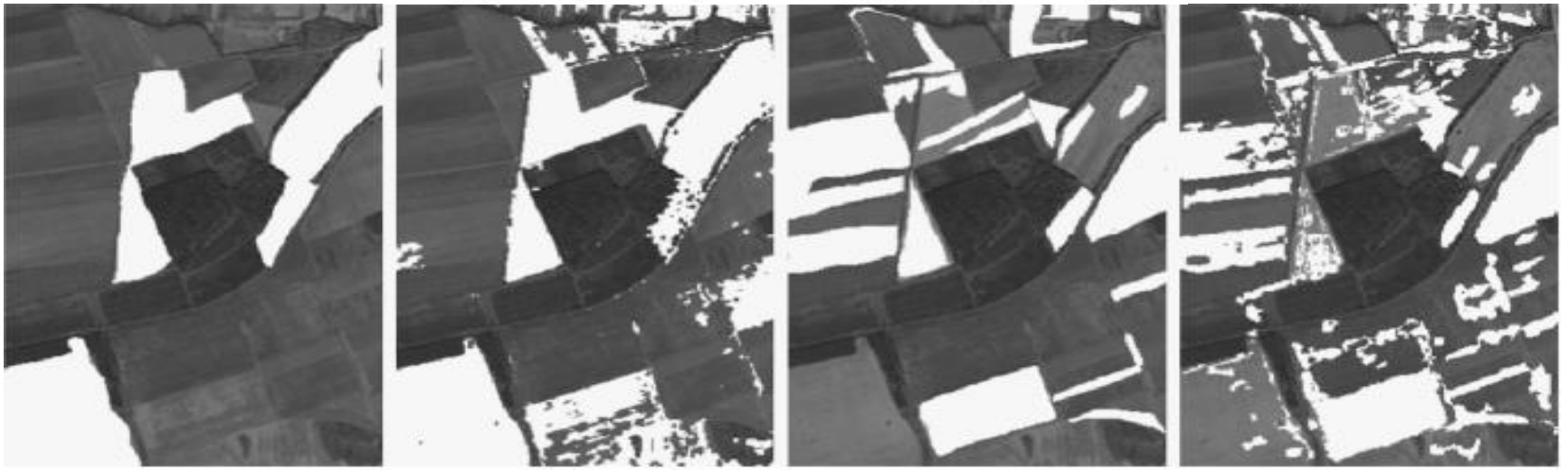

(c) AirChange GT (d) CXM result (e) Region PCC GT (f) FMRF result

Image	AirChange GT					
	CXM			FMRF		
	Pr	Rc	Fr	Pr	Rc	Fr
Szada/1	**36.5**	**58.4**	**44.9**	32.6	54.3	40.8
Archive	**47.0**	62.7	**53.7**	27.9	**71.2**	40.1
Forest	**61.7**	**93.4**	**74.3**	13.4	18.5	15.6

Image	Region PCC GT					
	CXM			FMRF		
	Pr	Rc	Fr	Pr	Rc	Fr
Szada/1	34.5	50.3	40.9	**45.6**	**69.0**	**54.9**
Archive	51.4	32.7	40.0	**59.1**	**72.2**	**65.0**
Forest	31.3	39.1	34.8	**61.5**	**69.6**	**65.3**

Orientation selective models for aerial image segmentation

A. Manno-Kovacs and T. Sziranyi, "Orientation-selective building detection in aerial images", ISPRS Journal of Photogrammetry and Remote Sensing, vol. 108, pp. 94-112, 2015.

Orientation sensitive building detection

- Extracting MHEC feature point set
- Contribution: Main orientation(s) of urban area:
  - Histogram of φ_i values (main orientation for *i*th feature point):

$$\vartheta(\varphi) = \frac{1}{K}\sum_{i=1}^{K} H_i(\varphi) \quad \text{, where} \quad H_i(\varphi) = \begin{cases} 1, & \text{if } \varphi_i = \varphi \\ 0, & \text{otherwise} \end{cases}$$

  - Correlating $\vartheta(\varphi)$ to bimodal Gaussian function(s) (peaks: θ, $\theta+90$)

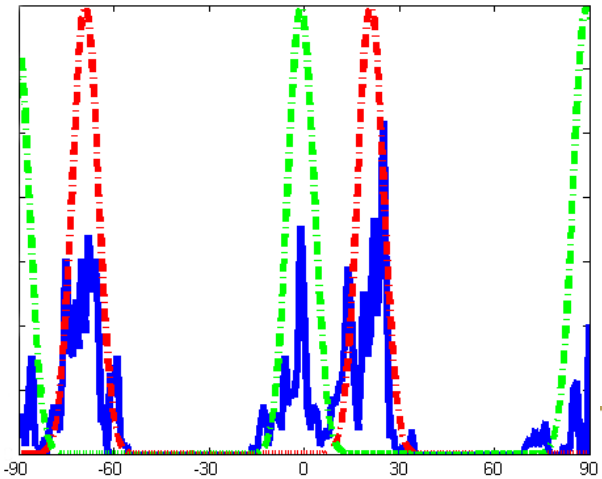

Orientation sensitive building detection

- Feature points are classified with K-means
- Pixels are clustered with k-NN clustering (k=7)
- Enhance edges only in the given direction: MFC (Zingman, 2014)


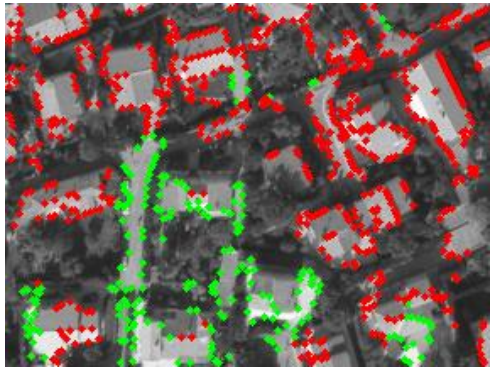
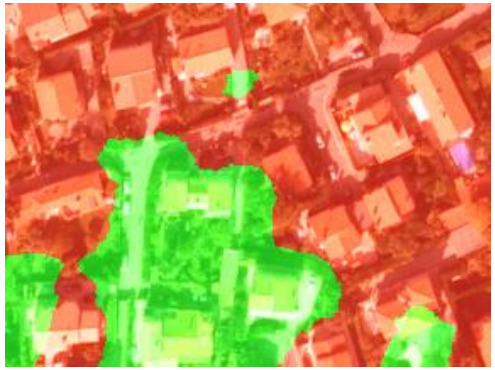

- Fusion of feature points; connectivity information (color + edges) and shadow blobs are merged for region based contour detection


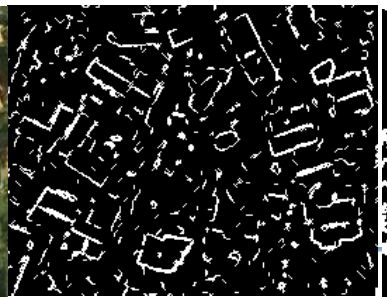
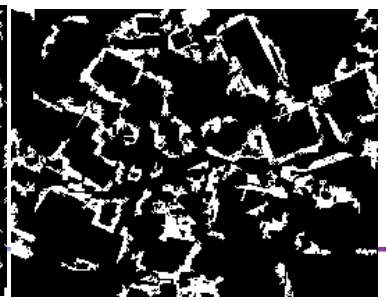
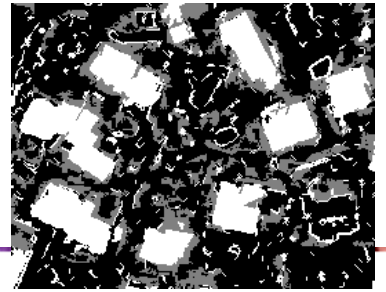


Orientation sensitive building detection - Results

Database	Performance								
	bMBD [19]			GrabCut [21]			Proposed OSBD		
Image name	F-score	Recall	Precision	F-score	Recall	Precision	F-score	Recall	Precision
image1	86.6%	87.7%	85.5%	88.1%	89.4%	86.9%	**94.0%**	91.4%	96.7%
image2	80.7%	78.6%	83.0%	89.1%	93.6%	85.0%	**93.5%**	91.2%	95.9%
image3	82.6%	81.0%	84.3%	90.4%	93.5%	87.5%	**90.6%**	87.6%	93.9%
image4	72.5%	90.7%	60.3%	**92.4%**	95.8%	89.3%	91.4%	87.1%	96.0%
image5	62.9%	72.6%	55.5%	81.1%	89.2%	74.4%	**81.8%**	74.6%	90.5%
image6	67.3%	78.9%	58.6%	75.9%	95.9%	62.8%	**77.4%**	66.7%	92.3%
Average	75.4%	81.6%	71.2%	86.2%	**92.9%**	81.0%	**88.1%**	83.1%	**94.2%**

Image data set:

- 230 buildings;
- VHR optical satellite;
- 0.61 m/pixel.

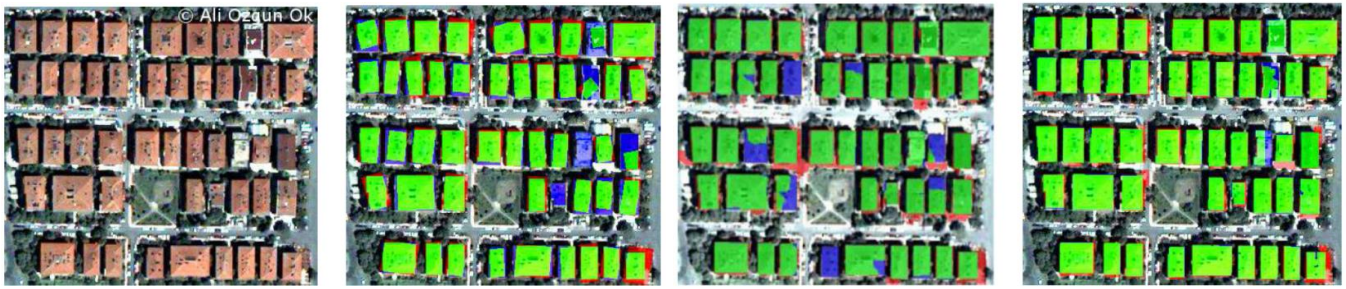

Vaihingen data set

- 306 buildings;
- Aerial photos;
- 0.09 m/pixel.

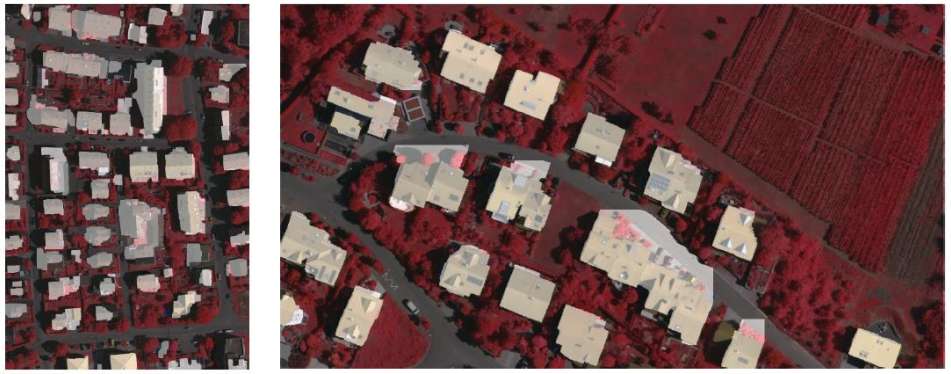

Orientation sensitive building detection - Results

- Experiments (***Outperforms the compared methods***):
  - Quantitative: only object level performance (building location)
  - Comparison with other state-of-the-art methods
  - Multidirectional dataset: 5 image sets, 453 buildings, 0.5 – 2.5 m/pixel.

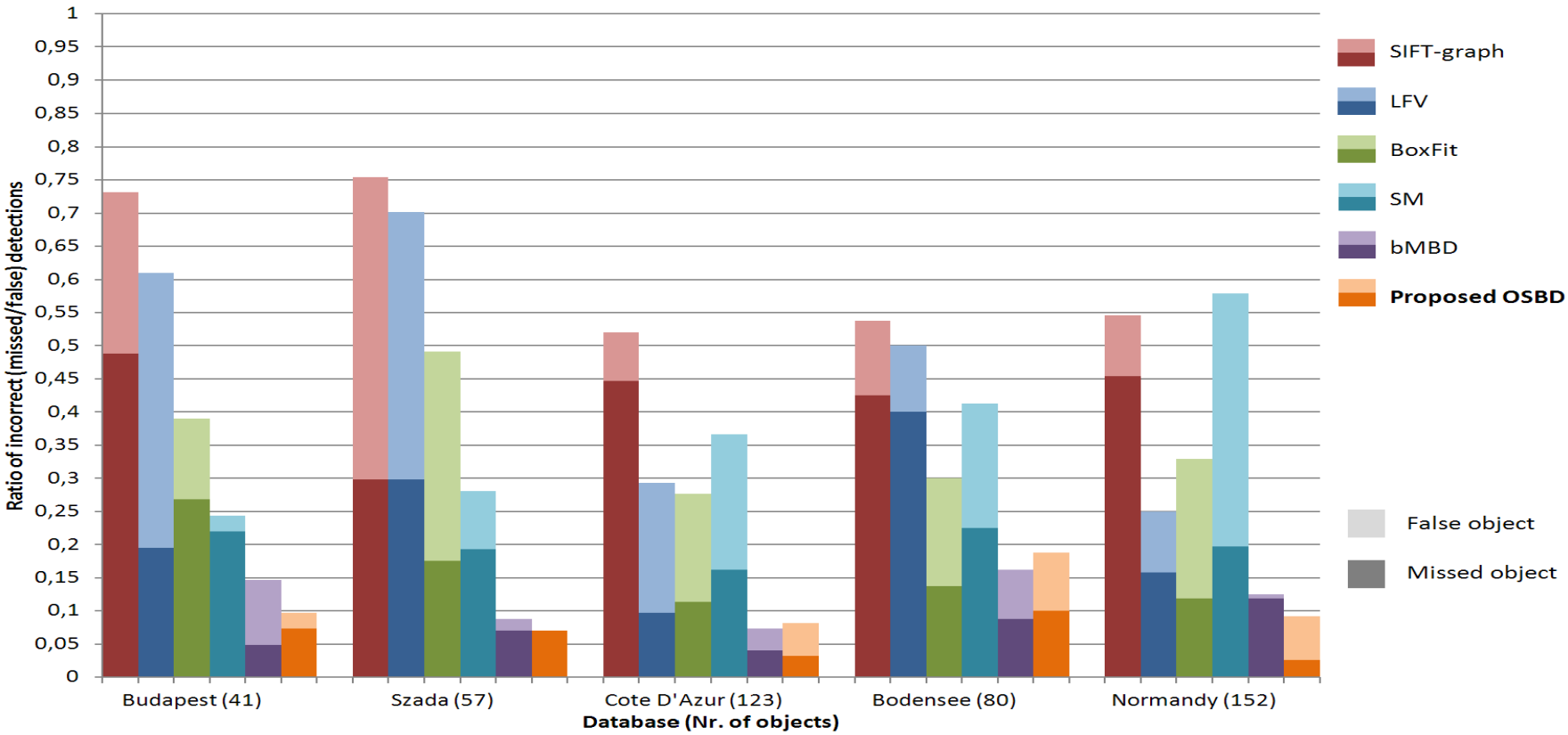

Thank You for your Attention!

Applications areas

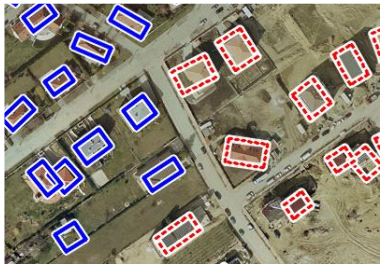

Remote sensing

Scene analysis, change detection and 3D reconstruction

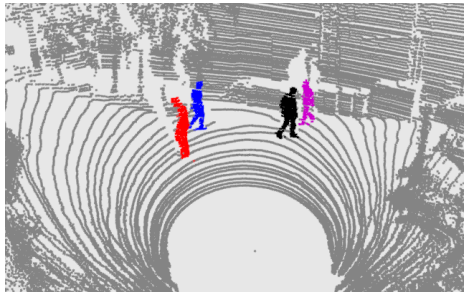

Security systems

people tracking, biometric identification, activity recognition

4D visualization

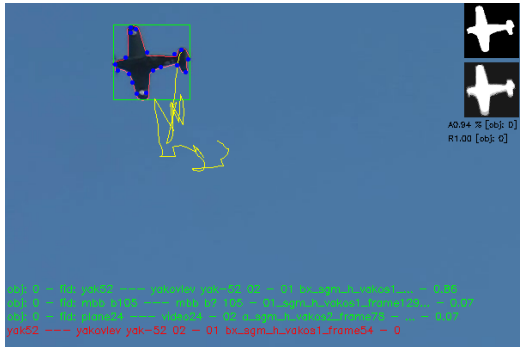

Large scale surveillance

Airborne and terrestrial multi target tracking and target identification

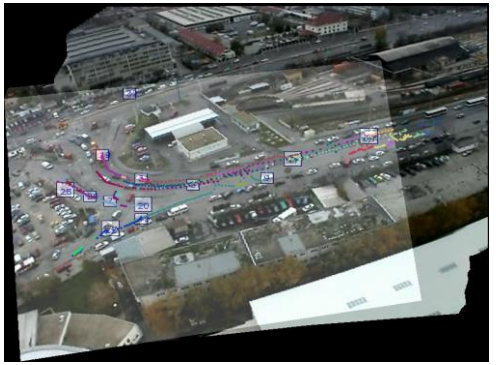

2D and 3D image sources

Aerial image

Satellite image

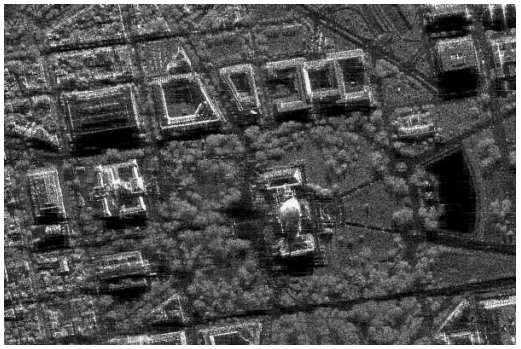

Radar (TerraSAR)

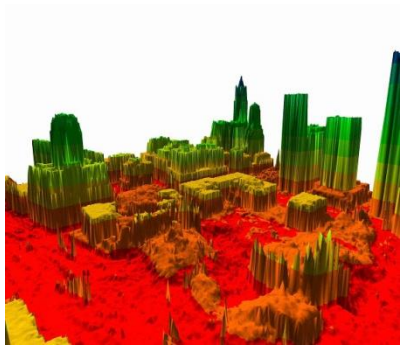

Lidar point cloud

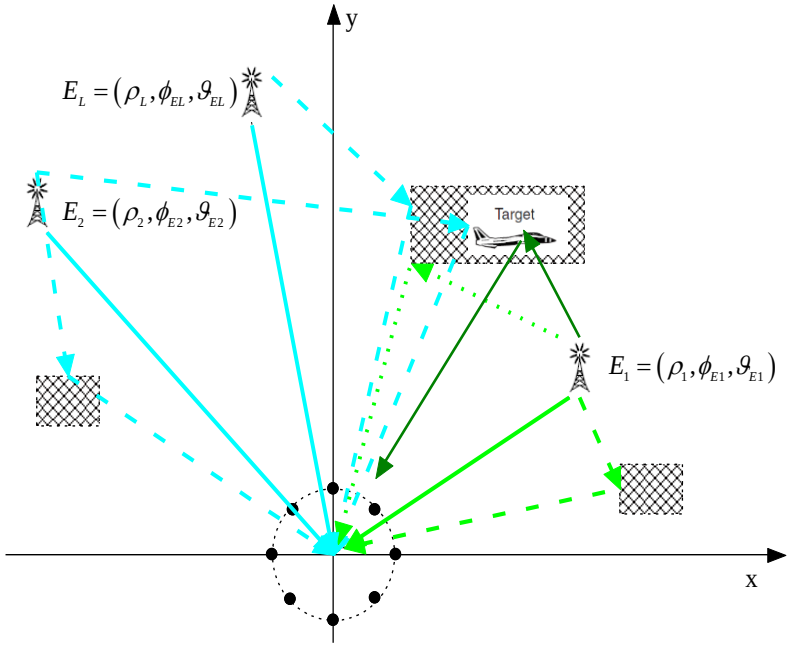

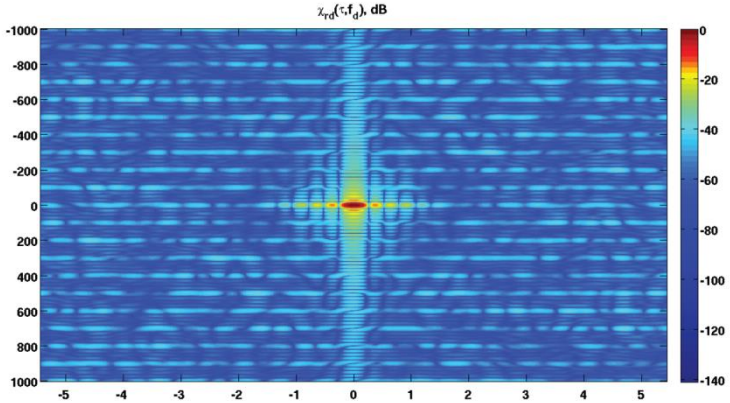

Passive radar

Main topics

- Pattern recognition, clustering
- 3D geometry
- Remote sensing
- Lidar measurements
- Mobil and robot vision and sensing devices
- Biometrical identification and featuring
- UAV imaging

Current projects

- **Pro-Active** (***EU FP7 Security***, 2012-15)
  - **PRedictive reasOning and multi-source fusion empowering AntiCipation of attacks and Terrorist actions In Urban EnVironmEnts**
- **DUSIREF** (***European Space Agency***, 2013-16)
  - Remote sensing, 2D and 3D data fusion and modelling - aerial and satellite image classification with change detection
- **MAPIS** (EDA, 2015-17)
  - radar image processing and recognition, aerial remote sensing, change and event detection